Characterization of Langasite ($La_3Ga_5SiO_{14}$) system's sintered body

Il Hyoung Jung, Kyoung Joo*, Kwang Bo Shim* and Keun Ho Auh*
Department of Ceramic Engineering, Hanyang University, Seoul, Korea 133-791
*Ceramic Processing Research Center, Seoul, Korea 133-791

Abstract Langasite is a new piezoelectric material which is similar to quartz in its acoustic behaviours. In this study, pure Langasite and Langasite family group powders were synthesized by the solid state reaction in air. And then diffusion of synthesized powders were controlled by B and C ions in the $A_3B_5CD_{14}$ structure. Dielectric constant and lattice anisotropy of Langasite and family group were measured to be 17, 22~27 in the range of 1 kHz to 13 MHz and about 1.6 , respectively.

1. Introduction

Rapid progress of electronic technologies required the development of new piezoelectric materials with smaller size, lower impedance and wide passband. For designing a filter devices, Langasite is a new piezoelectric material which exhibit piezoelectric properties intermediate between those of quartz and lithium tantalate[1-3].

Langasite is a crystal which has been grown and investigated for laser devices since the 1980s in Russia[4-5]. Its promise as a material for SAW, BAW and resonator devices was determined from it's acoustic characteristics[6-11]. It was a single oxide compound of the ternary system, and was grown by the Czochralski method. Langasite has a trigonal structure which belongs to point group 32, space group P321, and is isostructural to $Ca_3Ga_2Ge_4O_{14}$. There are four kind of cation sites in this structure and represent by the $A_3BC_3D_2O_{14}$. As shown in Fig. 1, A and B was located in a decahedral site and octahedral site, respectively. While C and D on the other hand was located in tetrahedral site. In case of Langasite, La^{3+} occupies the A sites, Ga^{3+} occupies the B, C and half of the D sites, and Si^{4+} half of the D sites, respectively[12-16].

In this present study, we will demonstrate the successful synthesis of Langasite and Langasite family group powders by the solid state reaction in air. Characteristics of

sintered body which made from synthesized powders will be discussed by dielectric properties and physical properties.

2. Experimental procedures

The starting materials for the synthesis were used 99.99% oxide of La_2O_3, Ga_2O_3 SiO_2, Ta_2O_5 and GeO_2. The mixed materials by dry mixing were heated in alumina crucible at temperature range of 1000 ~ 1400℃ in air. And then synthesized powders were identified using the powder x-ray diffractometer. In order to study diffusion process for synthesizing material such as $La_3Ga_5SiO_{14}$, $La_3Ta_{0.5}Ga_{5.5}O_{14}$ and $La_3Ga_5GeO_{14}$, pellet of La_2O_3, Ga_2O_3 and GeO_2 which was pressed from powders, was stacked together and sintered at various temperatures. The surfaces of sintered plates, which was in contact with each other during sintering, was analyzed by the energy dispersive x-ray spectroscopy and wavelength dispersive x-ray spectroscopy.

A physical and dielectric properties of sintered body with disc shape were investigated by the x-ray diffractometer and impedance analyzer.

3. Results and discussion

As shown in Fig.2 and Fig.3 , XRD results needed to investigated the secondary phases and homogeneous single phase for calcination. In Fig.2 where $La_3Ga_5SiO_{14}$ was calcined at 1400℃ for 5h to synthesize powders through the solid state reactions, it was found that $La_3Ga_5SiO_{14}$ phase began forming at 1100℃ while a secondary phase and unreacted phase, La_2O_3, Ga_2O_3, $LaGaO_3$ were mainly detected. These powders dissipating and then the quantity of secondary phase, $LaGaO_3$ was found to decrease with time and temperature. But main peak decreased with increasing temperature and time. It was considered that evaporation of gallium suboxide had an effect on synthesis of Langasite powders. So, the calcination condition for synthesis of pure $La_3Ga_5SiO_{14}$ with no other compound was found to be at 1400℃ for 5h. As shown in Fig.3 , $La_3Ta_{0.5}Ga_{5.5}O_{14}$ single phases were synthesized in same conditions. In case of synthesis such as Langasite and Langasite family group, synthesized powders were reacted the alumina crucible. But, in Fig.4, $La_3Ga_5GeO_{14}$ was not reacted the alumina crucible because $La_3Ga_5GeO_{14}$ phase was synthesized at lower temperature, 1300℃ compare with other Langasite family group and Langasite powders.

In Fig. 5, diffusion process for synthesizing material such as $La_3Ga_5SiO_{14}$, $La_3Ta_{0.5}Ga_{5.5}O_{14}$ and $La_3Ga_5GeO_{14}$, pellet of La_2O_3, Ga_2O_3 and GeO_2 which was pressed from powders, was stacked together and sintered at 1100℃, 1300℃. The

surfaces of sintered plates, which was in contact with each other during sintering, was analyzed by the energy dispersive x-ray spectroscopy and wavelength dispersive x-ray spectroscopy. As the above results, diffusion reaction occurs on the interface of Ga_2O_3 and GeO_2 while it was not observed on that of Ga_2O_3 and La_2O_3. Ga and Ge ions were main diffusion species and thus when $La_3Ga_5GeO_{14}$ is synthesized, Ga_2O_3 and GeO_2 is thought to react with one another previous to the full synthesis of $La_3Ga_5GeO_{14}$.

In Fig. 6, dielectric constant of polycrystalline Langasite had a 17～18 and Langasite family group had a 22～27 in the range of 1 kHz to 13 MHz. Also, phase transition was not observed up to around the melting temperature.

As shown in Fig. 7 and Table 1, the lattice constants of $La_3Ga_5SiO_{14}$, $La_3Ta_{0.5}Ga_{5.5}O_{14}$ and $La_3Ga_5GeO_{14}$ were measured to be a=8.1455, 8.228, 8.2009Å and c=5.102, 5.124, 5.1142Å, respectively. Also, crystal structure and lattice anisotropy of Langasite family group were similar to those of Langasite.

4. Summary

Pure Langasite and Langasite family group powders were synthesized by the solid state reaction in air. And then diffusion of synthesized powders were controlled by B and C ions in the $A_3B_5CD_{14}$ structure. In case of Langasite family group synthesis, we can see that Ga^{3+} and Ge^{4+} play an important role from the results of EDS and WDS.

The lattice constants of $La_3Ga_5SiO_{14}$, $La_3Ta_{0.5}Ga_{5.5}O_{14}$ and $La_3Ga_5GeO_{14}$ were measured to be a=8.1455, 8.228, 8.2009Å and c=5.102, 5.124, 5.1142Å, respectively. Also, crystal structure and lattice anisotropy of Langasite family group were similar to those of Langasite.

Dielectric constant of polycrystalline Langasite had a 17～18 and Langasite family group had a 22～27 in the range of 1 kHz to 13 MHz. And then, phase transition was not observed up to around the melting temperature.

References

[1] M.F.Dubovik, I.A.Andreyev, Yu.S.Shmaly "Langasite($La_3Ga_5SiO_{14}$) an optical piezoelectric:Growth and properties," IEEE International Frequency Control Symposium, 43-47 (1994).

[2] K.Shimamura, H.Takeda, T.Kohno, T.Fukuda "Growth and characterization of lanthanum gallium silicate $La_3Ga_5SiO_{14}$ single crystals for piezoelectric applications,"

J.Crys.Growth, 163, 388-392, (1996).

[3] H.Takeda, K. Shimamura, T.Kohno, T.Fukuda "Growth and characterization of $La_3Nb_{0.5}$ $Ga_{5.5}O_{14}$ single crystals," J.Crys.Growth, 5284,(1996).

[4] S.Laffey, M.Hendrickson and John R.Vig " Polishing and etching Langasite and quartz crystals," IEEE International Frequency Control Symposium, 245-250, (1994).

[5] I.M.Silvestrova, V.V.Bezdelkin, P.A.Senyushenkov, Yu.V.Pisarevsky " Present stage of $La_3Ga_5SiO_{14}$ - Research," IEEE International Frequency Control Symposium, 348-350, (1993).

[6] G.D.Mansfeld " Measurement of Acoustic Wave Attenuation in $La_3Ga_5SiO_{14}$ using HBAR technique," IEEE International Frequency Control Symposium, 35-39, (1994).

[7] C.Damhansen, PM.Johansen and VM.Fridkin " Photorefractive grating formation in piezoelectric $La_3Ga_5SiO_{14}$-Pr^{3+} crystals," Appl.Phys.Letters, Vol69,No14, 2003-2005, (1996).

[8] M.Sato, K.Moroishi and S.Ishigami "Filter and Resonator using Langasite," IEEE International Frequency Control Symposium, 379-383, (1996).

[9] H.J.Eichler, D.Ashkenasi, H.Jian and A.A.Kaminski " Acentric disordered Nd^{3+}: $La_3Ga_5SiO_{14}$ crystal. A broadband luminescence material with high thermal conductivity to generate picosecond Laser pulses," Phys.stat.sol. 146, 833 (1994).

[10] H.Satoh and A.Mori "Surface Acoustic Wave propagation characteristics on a Langasite crystal plate," Jpn.J.Appl.Phys.,Vol.36, 3071-3073 (1997).

[11] W.Laprus and E.Danicki " Piezoelectric interfacial waves in Lithium Niobate and other crystals," J.Appl.Phys. 81(2), (1997).

[12] T.Fukuda, K.Shimamura, T.Kohno, H.Takeda and M.Sato "新壓電結晶ランガサイト" 日本結晶成長學會誌,Vol.22 No.5 (1995).

[13] T.Sato, A.Nisikato and Y.Shimizu "$La_3Ga_5SiO_{14}$ 基板彈性表面波の 轉搬特性" (1996).

[14] M.Koshiba and N.Shichishima "有限要素法とモード結合理論を用いた" (1996).

[15] T.Kohno, K.Moroishi, M.Sato K.Shimamura and T.Fukuda "ランガサイトの育成とデバイスへの應用" (1996).

[16] M.Takeuchi and K.Yamanouchi "NSPUDT orientation of a $La_3Ga_5SiO_{14}$ substrate," 第26回EM Symposium, 69-72.

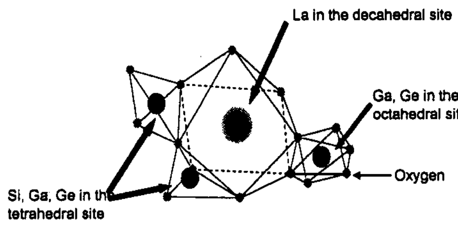

Fig.1 Configuration of Langasite crystal structure

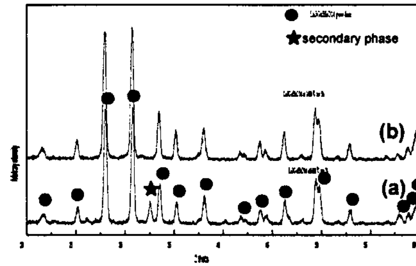

Fig.2 XRD pattern of $La_3Ga_5SiO_{14}$ at 1400℃ for (a) 2h, (b) 5h.

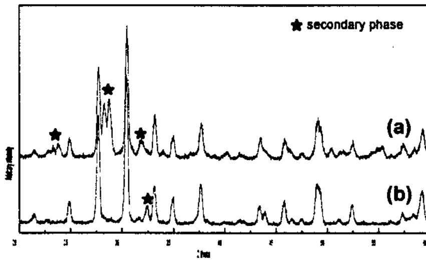

Fig.3 XRD pattern of $La_3Ta_{0.5}Ga_{5.5}O_{14}$ at 1400℃ for (a) 5h, (b) 10h.

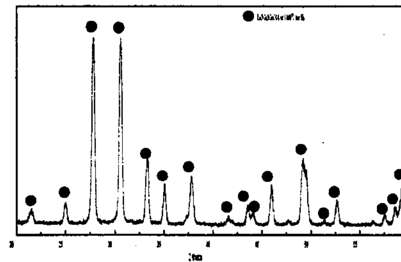

Fig.4 XRD pattern of $La_3Ga_5GeO_{14}$ at 1300℃ for 5h.

Fig.5 Diffusion species of surfaces of sintered plate was analyzed by the WDS.

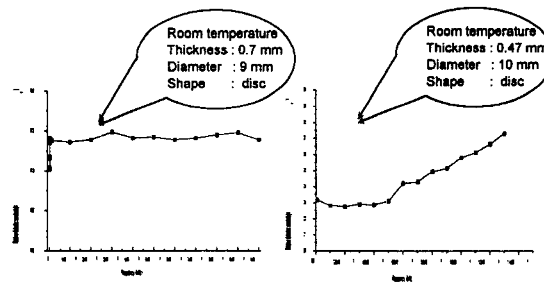

Fig.6 Dielectric constant of $La_3Ga_5SiO_{14}$ and La_3 -Ga_5GeO_{14} were measured by impedance analyzer.

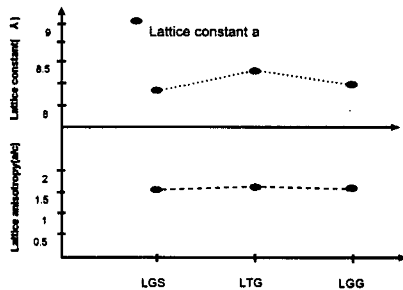

Fig.7 Lattice constants and lattice anisotropy of Langasite and family group.

Table 1. Lattice constants and lattice anisotropy of Langasite and family group.

Phase	a(Å)	c(Å)	Lattice anisotropy (a / c)
$La_3Ga_5SiO_{14}$	8.1455	5.102	1.596
$La_3Ta_{0.5}Ga_{5.5}O_{14}$	8.228	5.124	1.605
$La_3Ga_5GeO_{14}$	8.2009	5.1142	1.604

Chemical vapor deposition of β-SiC film on Si substrate using hexamethyldisilane/H_2 gas system

Won Jae Yang
Department of Ceramic Engineering, Hanyang University, Seoul 133-791, Korea
Yong Sun Chung and Keun Ho Auh
Ceramic Processing Research Center, Hanyang University, Seoul 133-791, Korea

Abstract

A behavior of the surface of Si substrate was investigated by changing the deposition process of a substrate temperature and reactor pressure. And β-SiC thin film was successfully deposited on a (100) Si substrate by a chemical vapor deposition method. The selectivity of SiC deposition between a Si substrate and a mask material was improved by introducing HCl gas.

Introduction

Cubic SiC(β-SiC) has excellent electrical properties like as a high saturated electron drift velocity, a high electron mobility and a high thermal conductivity[1]. Also, it has wide band gap energy more than 2.0 eV[2-3]. Therefore, it is a favorable semiconductor material for high temperature, high power and high speed electronic devices. However, it is necessary to have a mirror-like surface of SiC film for the application of electronic devices[4]. Also, the selective deposition is a useful method to achieve the patterning because it is difficult to use a general wet etching technique for patterning due to a chemical stability of SiC.

Chemical vapor deposition (CVD) has been successful and reliable method for growth of SiC thin film on both Si and SiC substrates[5]. Using single precursor such as tetramethylsilane ($Si(CH_3)_4$), hexamethyldisilane ($Si_2(CH_3)_6$) and methyltrichlorosilane (CH_3SiCl_3), a low temperature deposition was easily achieved in contrast to the deposition using separate source gas such as silane (SiH_4) and hydrocarbons (methane, propane, etc.). In addition, a single precursor may be effective for forming Si-C bonds because of containing Si-C direct bond in origin molecules[6].

In this study, the behavior of Si surface and the condition of SiC deposition for HMDS precursor was investigated by changing the deposition process, mainly a substrate temperature and a reactor pressure. Also, the selectivity of SiC deposition was investigated between a Si substrate and a mask material.

Experimental Procedures

A low pressure chemical vapor deposition system was used to deposit SiC thin film. CVD system consisted of hot-wall type horizontal reaction tube with SiC heater. Hexamethyldisilane ($Si_2(CH_3)_6$) was used as a single precursor for SiC deposition. <100> oriented Si wafer was used as a substrate and SiO_2 and Si_3N_4 were used as mask materials. Flow rate of source gas was determined by flow rate of carrier H_2 gas, vapor pressure of liquid source and temperature of bubbler containing liquid HMDS precursor. Bubbler temperature was held at 4℃ using ice water bath. The vapor pressure of liquid source at this temperature was about 9 torr. The flow rate of carrier H_2 gas through a bubbler was varied from 1 to 10 sccm. The flow rate of atmosphere H_2 gas direct to a reactor was kept at 1,000 sccm. The flow rate of HCl gas was varied from 20 to 200 sccm. Substrate temperature was maintained between 1100 and 1200℃ and reactor pressure was held between 30 and 50 torr. Typical deposition time was 20 min. When the precursor flowed as a pulse type, the precursor was introduced intermittently for 10 min.

Results and Discussions

When all processes were done under the reduced pressure, the deposited SiC film was easily stripped from Si substrate and Si substrate was extremely etched, as shown in Fig. 1. Also, a fiber-like growth on the etched surface was observed. It was confirmed that the randomly oriented SiC film was grown, showing higher intensity of (111) peak, as shown in Fig. 2. It was considered that Si substrate was damaged before the deposition began.

Therefore, to investigate a behavior of Si surface, Si substrate was heated at 1100, 1150 and 1200℃, respectively, without supplying the source gas. In this case, Si surface was changed at the substrate temperature above 1150℃. Fig. 3 shows the microstructure of Si surface heated at 1200℃. Si surface was extremely damaged and a fiber-like growth was observed as similar to Fig. 1. From the Si : O ratio of 1 : 2 composition by WDS analysis, those phases were identified as SiO_2 phase. It was considered that formation of SiO_2 was mainly dependent on an oxygen gas, not a substrate temperature.

Therefore deposition process, especially the chamber pressure, was modified. In previous experiment, all processes including heating, deposition and cooling were carried out under the reduced pressure. However, in modified process, heating and cooling were carried out at the atmospheric pressure with a flow of Ar gas and deposition was carried out at the reduced pressure.

Using this modified process, Si substrate was not damaged and the stable interface relationship was observed between the deposited film and the Si substrate. And, the deposited film showed a mirror-like surface. Also, by WDS analysis, it was confirmed that SiC film of the stoichiometric composition was grown on the Si substrate. Cross-sectional view of the film deposited at 1100℃ was shown in Fig. 4.

However, a few of the defects of fiber-like growth were appeared on the surface of the film deposited at the substrate temperature above 1150℃. By WDS analysis, it was determined as SiO_2 phase like as a previous case. Therefore, typical substrate temperature was chosen as 1100℃.

By X-ray diffraction pattern, the deposited films were identified as β-SiC and preferentially grown along the <111> direction. Fig. 5 shows XRD patterns of the deposited films. Fig. 6 shows the AFM images of β-SiC thin film deposited at 1100 and 1200℃. In both case, the average roughness of β-SiC surface was 23.8Å and 22.7Å, respectively.

For the selectivity of SiC deposition, HCl gas that can etch Si nuclei was added to HMDS/H_2 gas mixture. To increase the etch rate of Si nuclei on a mask and decrease the deposition rate of SiC film on a Si substrate, the precursor was introduced as a pulse type and HCl gas was introduced continuously. As HCl gas flow rate increased, both SiC film thickness on a Si substrate and a mask area decreased. But, the deposition rate on a Si substrate was faster than that on a mask area. It was confirmed that the selectivity of SiC deposition was improved by introducing HCl gas. Fig. 7 shows the SEM micrographs of the SiC film deposited at HCl gas of 200 sccm.

Summary

A behavior of Si surface was investigated. SiO_2 fiber growth was observed on Si surface because an oxygen gas was introduced unintentionally. Therefore, by modifying the deposition process, the optimum condition of a substrate temperature for SiC deposition using HMDS/H_2 gas system was determined as 1100℃. The interface relationship between SiC film and Si substrate was stable and SiC film showed a mirror-like surface. The selectivity of SiC deposition on a Si substrate and a mask

area was improved by introducing HCl gas.

References

[1] S. Nishino, H. Suhara, H. Ono and H. Matsunami, *J. Appl. Phys.*, **61**(10) 4889 (1987).

[2] J. A. Powell, L. G. Matus and M. A. Kuczmarski, *J. Electrochem. Soc.*, **134**(6) 1558 (1987).

[3] H. Nagasawa and Y. Yamaguchi, *J. Crystal Growth*, **115** 612 (1991).

[4] K. Shibahara, S. Nishino and H. Matsunami, *J. Crystal Growth*, **78** 538 (1986).

[5] N. Nordell, S. Nishino, J.-W. Yang, C. Jacob and P. Pirouz, *J. Electrochem. Soc.*, **142**(5) 565 (1995).

[6] G. Krotz, W. Legner, G. Muller, H. W. Grueninger, L. Smith, B. Leese, A. Jones and S. Rushworth, *Mat. Sci. & Eng. B*, **29** 154-159 (1995).

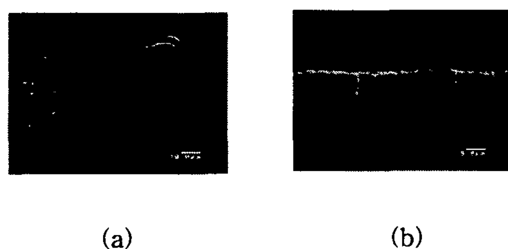

(a) (b)

Fig. 1. SEM micrographs showing the damaged Si surface and the SiC layer deposited at 1150℃ and 50 torr : (a) surface morphology and (b) cross-sectional view.

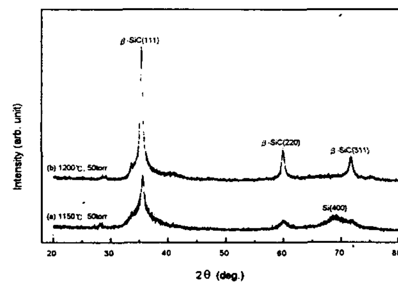

Fig. 2. XRD patterns of the films deposited at various substrate temperatures. Note that all processes including heating, deposition and cooling were carried out under the reduced pressure.

(Atomic %)

	Region A	Region B	Region C
Si	29.6	27.94	34.37
O	67.96	67.54	60.45
C	2.44	4.52	5.18

Fig. 3. SEM micrograph showing the surface morphology of Si substrate heated at 1200℃ without supplying the source gas. The compositions of the phases on Si surface by WDS analysis were, also, shown.

Fig. 4. SEM micrograph showing the cross-sectional view of β-SiC film deposited at 1100℃

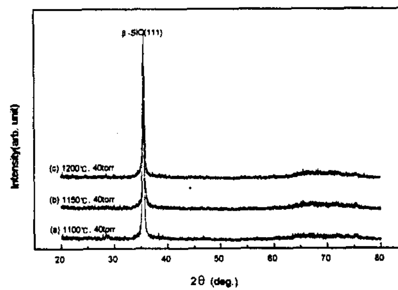

Fig. 5. XRD patterns of the films deposited at various substrate temperatures. Note that heating and cooling were carried out at the atmosphere pressure and deposition was carried out at the reduced pressure.

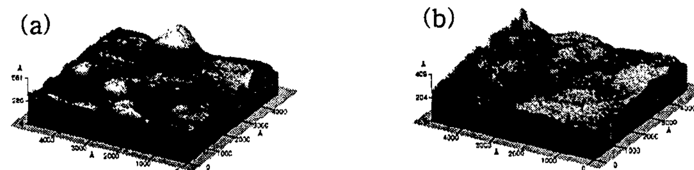

Fig. 6. AFM images of β-SiC thin film deposited at (a) 1100℃ and (b) 1200℃.

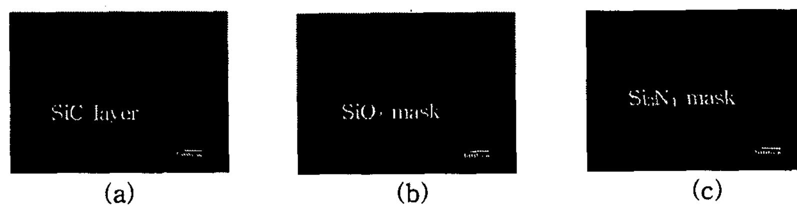

Fig. 7. SEM micrographs showing the SiC film deposited on (a) Si substrate, (b) SiO_2 mask and (c) Si_3N_4 mask at HCl gas of 200 sccm.